NASA Technical Paper 1883

Relationship Between the Ideal Tensile Strength and the Friction Properties of Metals in Contact With Nonmetals and Themselves

Kazuhisa Miyoshi and Donald H. Buckley

SEPTEMBER 1981

NASA

NASA Technical Paper 1883

Relationship Between the Ideal Tensile Strength and the Friction Properties of Metals in Contact With Nonmetals and Themselves

Kazuhisa Miyoshi and Donald H. Buckley
Lewis Research Center
Cleveland, Ohio

NASA
National Aeronautics
and Space Administration

Scientific and Technical
Information Branch

1981

Summary

An investigation was conducted to define the relationships between the ideal tensile strength and friction properties of elemental metals in contact with diamond, boron nitride, silicon carbide, manganese-zinc ferrite, and with the metals themselves. An estimate of the ideal uniaxial tensile strength σ_{max} for metals was obtained from equilibrium surface energy and interplanar spacing of the planes perpendicular to the tensile axis, and the Young's modulus of eleasticity.

The coefficients of friction for metals are all related to the ideal tensile strength of the metals. The higher the strength of the metal, the lower the coefficient of friction.

Introduction

In the 1940's Pauling recognized differences in the amount of the *d* bond character associated with transition metals (ref. 1). Since the *d*-valence bonds are not completely filled in the transition metals, the filling of the *d*-valence electron band in transition metals is responsible for physical and chemical properties such as cohesive energy, shear modulus, chemical stability, and magnetic properties. The greater the amount or the percentage of *d*-bond character that a metal possesses, the less active is its surface. The adhesion and friction of metals in contact with themselves can be related to the chemical activity of the metal surfaces (ref. 2). The *d*-bond character of the metal influences the adhesion and friction for metals in contact with diamond, pyrolytic boron nitride, silicon carbide, and manganese-zinc ferrite crystals, just as it does for metals in contact with themselves (refs. 3 to 6). The more active the metal, the higher the coefficient of friction.

We have proposed a mechanism for this behavior. All the metals examined in references 2 to 6 deformed very locally in a plastic manner and transferred to the surface of the nonmetallic materials or metals with sliding. Interfacial bonds are generally stronger than the cohesive bonds in the cohesively weaker metal.

On separation of the metallic and nonmetallic material in sliding, tearing and shearing fracture occurs generally in the metal, and the metal subsequently transfers to the nonmetallic material or the other contacting metal. It is, therefore, anticipated that the fracture, metal transfer, and metal wear would be related to chemical, physical, and the metallurgical properties and strength of metals. For example, the effect of chemical properties (such as affinity or activity) of the metal has been observed to play an important role in the metal transfer and form of metal wear debris, generated by fracture of cohesive bonds (ref. 5). In general, the less chemically active the metal, the less transfer to the nonmetallic material and the less the friction.

These data, however, were not clearly surveyed by physical properties or strength of materials (ref. 5). They were not related to mechanical properties such as hardness. The adhesion, friction, or fracture properties of metals in contact with metals or nonmetals should be understood as a function of their physical properties, such as tensile strength.

The objective of this paper is to investigate the relationship between the ideal tensile strength and the friction properties of metals in contact with metals and nonmetals.

All sliding friction experiments were conducted with light loads, 0.01 to 0.5 newton, at a sliding velocity 0.70, 0.77, or 3 millimeter per minute, in a high vacuum of 10^{-8} pascal and at room temperature. Frictional heating did not produce a measurable temperature rise. Experiments were conducted in this investigation with the metal pin specimens sliding on the nonmetal or metal flats. The radius of pin specimen was 0.79 millimeter.

Materials

Diamond. – Natural, single-crystal diamonds were used in these experiments. The {111} plane was parallel to the sliding interface. The specimens that were less than $\pm 2°$ of the low index {111} plane were used. The samples were in the form of flat platelets and had a mean surface area of about 30 square millimeters.

Pyrolytic boron nitride. – The boron nitride was a 99.99 percent pure compound of boron and nitrogen. Its hexagonal crystal structure has a *C*/2 layer spacing of 0.233 to 0.343 nanometer and a nearest neighbor spacing of 0.146 nanometer in the hexagonal lattice. The *C* direction was perpendicular to the sliding interface with the basal planes therefore parallel to the interface.

Silicon carbide. – The single-crystal silicon carbide platelets used were a 99.9 percent pure compound of silicon and carbon. Silicon carbide has a hexagonal close-packed crystal structure. The basal plane was parallel to the interface.

Manganese-zinc ferrite. – The single-crystal manganese-zinc ferrite platelets were 99.9 percent pure oxide. The crystal is that of spinels in which the oxygen ions are in a nearly close-packed cubic array. The {110} plane was parallel to the interface.

Metals. – Two groups of metals were used. One was all single crystals, and the other was all polycrystalline.

The single-crystal metals are used for the sliding friction experiments with pyrolytic boron nitride and with the metals themselves. The body-centered-cubic metals had the {110} plane on their surface parallel to the sliding interface. The face-centered-cubic metals had the {111} planes parallel to the sliding interface and the hexagonal metals had the {0001} surfaces parallel to that interface.

The polycrystalline metals are used for the experiments with diamond, silicon carbide, and manganese-zinc ferrite.

The titanium was 99.97 percent pure, the copper was 99.999 percent pure, and all the other metals were 99.99 percent pure in both single-crystal and polycrystalline forms.

Experimental Apparatus and Procedure

The apparatus and experimental procedures related to this paper have already been described in references 2 to 6.

Theoretical Strength of Solids

The generally accepted thinking on the fracture of solids is that of the ideal elastic solid or one which would exhibit elastic response to a load until such time as atomic separation takes place on a plane by overcoming the interatomic forces. At the atomistic level fracture occurs when bonds between atoms are broken across a plane and a new surface is created. This can occur by breaking bonds perpendicular to the fracture plane (fig. 1(a)) or by shearing bonds across the fracture plane (fig. 1(b)). Such behavior is expected in the case of an ideal crystalline solid. At this level the fracture criteria are simple: fracture occurs when the local stress builds up either to the theoretical cohesive strength or to the theoretical shear strength. In this paper the theoretical cohesive strength will be discussed.

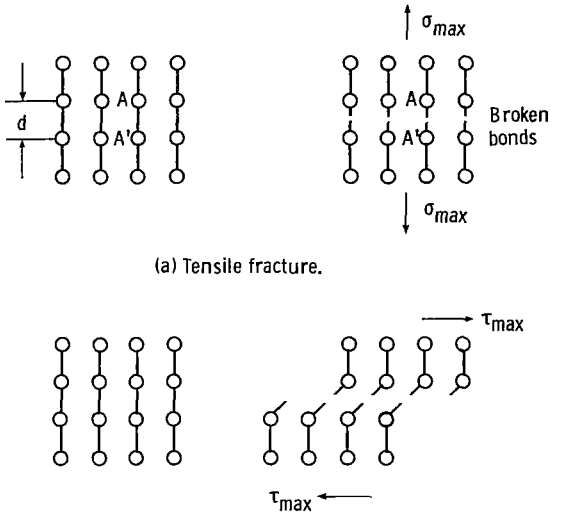

(a) Tensile fracture.

(b) Shear fracture.

Figure 1. - Fracture viewed at the atomistic level in terms of breaking of atomic bonds.

The calculation of the theoretical cohesive strength of an ideal elastic solid is based on the proposition that all the energy of separation is available for the creation of two new surfaces; the only expenditure in creating these two surfaces is assumed to be the surface energy. When the atoms A and A′ in figure 1(a) are pulled apart, the stress required to separate the planes is the ideal (or theoretical) tensile strength (σ_{max}), and, when that strength is reached, the bonds are broken. The ideal uniaxial tensile strength is then given by the equation

$$\sigma_{max} = \sqrt{\frac{E\gamma}{d}} \tag{1}$$

where E is Young's modulus, γ is the surface energy per unit area, and d is the interplanar spacing of the planes perpendicular to the tensile axis (refs. 7 to 11). In the equation the ideal strength of a solid is directly related to other macroscopic physical properties. The foregoing approach is equally applicable to any ideal solid.

Survey of Physical Properties

Surface energies of solid metals have been reported in the literatures (refs. 12 to 19). Table I is a compilation of surface energy values obtained from recommended values suggested by Tyson and Miedema (refs. 12 and 19). Miedema (ref. 19) estimated values at absolute zero temperature γ_0^s from values of the experimental surface energy and entropy. The surface energy at absolute zero

TABLE I. - VALUES FOR SURFACE ENERGY OF METALS IN THE SOLID STATE

Metal	Structure	Estimated surface energy, mJ/m^2	
		At room temperature,[a] γ^s	At absolute zero, γ_0^s
Al	[b]fcc	1150	1200
Ni		2400	2450
Cu		1800	1850
Rh		2700	2750
Pd		2050	2100
Ir		3050	3100
Pt		2500	2550
V	[c]bcc	2550	2600
Cr		2350	2400
Fe		2500	2550
Nb		2650	2700
Mo		2900	2950
Ta		3000	3050
W		3250	3300
Ti	[d]hcp	2000	2050
Co		2500	2550
Y		1050	1100
Zr		1900	1950
Ru		3000	3050
Re		3600	3650

[a]From Miedema (ref. 19).
[b]Face centered cubic.
[c]Body centered cubic.
[d]Hexagonal close packed.

TABLE II. - YOUNG'S (ELASTIC) MODULUS AND INTERPLANAR SPACING

Metal	Structure	Young's modulus, GPa	Lattice constant, nm	
			a	c
Al	[a]fcc	71.0	0.405	-----
Ni		193	.352	-----
Cu		126	.361	-----
Rh		372	.380	-----
Pd		123	.388	-----
Ir		527	.384	-----
Pt		171	.393	-----
V	[b]bcc	131	0.304	-----
Cr		243	.288	-----
Fe		210	.287	-----
Nb		105	.330	-----
Mo		327	.314	-----
Ta		181	.330	-----
W		397	.316	-----
Ti	[c]hcp	106	0.295	0.468
Co		206	.251	.407
Y		64.8	.365	.573
Zr		92.0	.323	.515
Ru		412	.270	.428
Re		461	.276	.446

[a]Face centered cubic.
[b]Body centered cubic.
[c]Hexagonal close packed.

temperature correlated with the thermochemical parameters for metals such as the electron density, the electronegativity, and heat of sublimation (refs. 13 and 19). Values at room temperature γ^s are calculated using the values of γ_0^s and the temperature dependence factors estimated by Miedema.

The surface energy data refer to mean surface. Anisotropy of surface energy is not considered in this paper (although it may be remarked that such anisotropy is usually small, with variations from the average of the order of 10 percent characteristic for cubic metals (refs. 20 and 22). Table II lists elastic moduli E and lattice constant of the metals used in this paper (from refs. 23 to 25). Young's modulus is for bulk, polycrystalline materials.

Correlation of Friction with the Ideal Tensile Strength

The values of the ideal tensile strength obtained from equation (1) are presented in table III. Three parameters listed in tables I and II were used for the calculations. The coefficients of friction for various pure elemental metals in contact with diamond (ref. 3), pryolytic boron nitride (ref. 4), silicon carbide (ref. 5), manganese-zinc ferrite (ref. 6), and the metals themselves (ref. 2) were taken from our previous studies.

Figure 2 presents the coefficients of friction as a function of σ_{max}. The data of these figures indicate a decrease in friction with an increase of the ideal tensile strength of the metal bond. There generally appears to be a strong correlation between friction and the ideal tensile strength of metals. The higher the tensile strength, the lower the friction.

The ideal tensile strengths of metals were calculated in the tensile directions of ⟨111⟩ for fcc and

TABLE III. - SIMPLE CALCULATIONS OF THE IDEAL TENSILE STRENGTH

	σ_{max}, GPa	σ_{max}/E	σ_{max}, GPa	σ_{max}/E	σ_{max}, GPa	σ_{max}/E
fcc	Tensile direction					
	⟨111⟩		⟨100⟩		⟨110⟩	
Al	19	0.27	20	0.28	24	0.34
Ni	48	.25	67	.35	68	.35
Cu	33	.26	47	.37	47	.37
Rh	68	.18	96	.26	97	.26
Pd	34	.28	47	.38	48	.39
Ir	85	.16	120	.23	122	.23
Pt	43	.25	61	.36	62	.36
bcc	Tensile direction					
	⟨110⟩		⟨100⟩		⟨111⟩	
V	39	0.30	47	0.36	62	0.47
Cr	53	.22	63	.26	83	.34
Fe	51	.24	60	.29	80	.38
Nb	35	.33	41	.39	54	.51
Mo	65	.20	78	.24	102	.31
Ta	48	.27	57	.31	75	.41
W	76	.19	90	.23	120	.30
hcp	Tensile direction					
	⟨0001⟩		⟨$11\bar{2}0$⟩		⟨$10\bar{1}0$⟩	
Ti	21	0.20	27	0.25	29	0.27
Co	36	.17	45	.22	49	.24
Y	11	.17	14	.22	15	.23
Zr	18	.20	23	.25	25	.27
Ru	54	.13	68	.17	73	.18
Re	61	.13	78	.17	83	.18

⟨110⟩ for bcc and ⟨0001⟩ for hcp metals. The correlation between the coefficient of friction and the ideal tensile strength of a metal may be due to the following reason:

According to the adhesion theory of friction as proposed by Bowden and Tabor (ref. 26), adhesion occurs at the contacting area between solids. All the slidings in this investigation involve such adhesion. The force F required to move the solid rider in a direction parallel to the surface of solid flat is determined by (1) the true interfacial contact area A and (2) the strength in the surficial region at the interface S. This may be written as

$$F = AS \tag{2}$$

where S is the force per unit of area which, acting in a direction tangential to the surface, is required to clear the surface region.

For an idealized case, it is assumed that the tip of the softer, solid rider is perfectly smooth and spherical. When the smooth surfaces of the rider (the radius of r) and the solid flat are pressed together with a load W, they will at first deform elastically according to Hertz's classical equations. The region of contact will be bounded by a circle of radius a, where

$$a = \left[\frac{3}{4} Wr\left(\frac{1-\sigma_1^2}{E_1} + \frac{1-\sigma_2^2}{E_2}\right)\right]^{1/3} \tag{3}$$

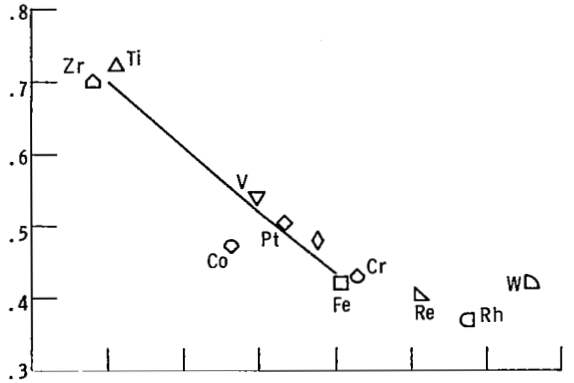

(a) Sliding material, single-crystal diamond {111} surface. Sliding direction, <1$\bar{1}$0>; sliding velocity, 3 mm/min; load, 0.05 to 0.3 N.

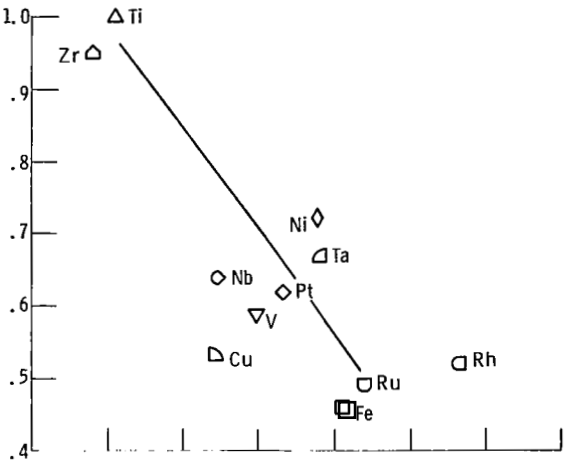

(b) Sliding material, pyrolytic boron nitride surface. Sliding velocity, 0.77 mm/min; load, 0.3 N.

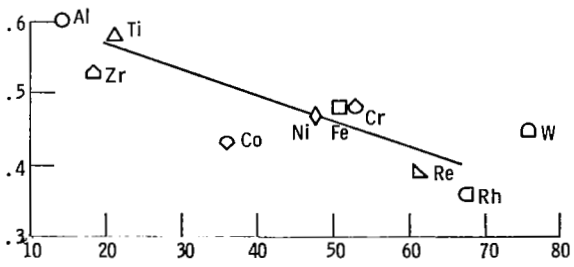

(c) Sliding material, single-crystal silicon carbide {0001} surface. Sliding direction, <10$\bar{1}$0>; sliding velocity, 3 mm/min; load, 0.05 to 0.5 N.

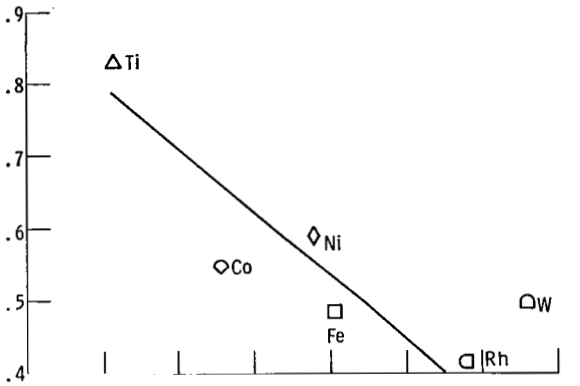

(d) Sliding material, single-crystal manganese-zinc ferrite {110} surface. Sliding direction, <1$\bar{1}$0>; sliding velocity, 3 mm/min; load, 0.3 N.

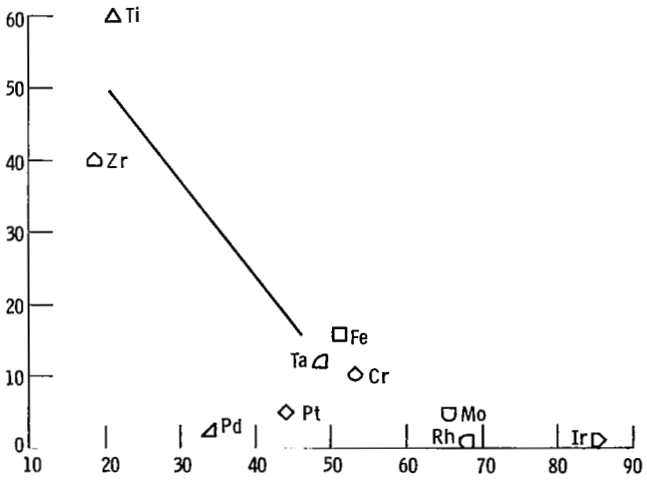

(e) Sliding material, metals themselves. Sliding velocity, 0.7 mm/min; load, 0.01 N.

Coefficient fo friction

Ideal tensile strength, σ_{max}, GPa

Figure 2. - Coefficients of friction as function of the ideal tensile strength of metals in contact with nonmetals and themselves. Tensile direction: <111> for fcc, <110> for bcc, and <0001> for hexagonal metals. Tests were conducted at room temperature at a vacuum pressure of 10^{-8} Pa.

where W is the load applied, E_1 and E_2 are Young's moduli of the rider and flat, respectively, and σ_1 and σ_2 are the corresponding values of Poisson's ratio. Since Poisson's ratio has a value of about 0.3 for most metals (ref. 23), this gives

$$a = 1.1\left[\frac{Wr}{2}\left(\frac{1}{E_1}+\frac{1}{E_2}\right)\right]^{1/3} \tag{4}$$

At this stage, the area of contact $A = \pi a^2$ is a function of $E_1^{-2/3}$ when E_2 is much greater than E_1.

In the actual case it is almost impossible to obtain perfectly smooth surfaces. Consequently, the fine surface irregularities will be deformed plastically while the bulk of the underlying metal will deform elastically. This means that the plastic deformation will occur at very local areas such as the tips of the surface asperities. The apparent area of contact will still deform essentially elastically. Figure 3 presents an example of the relationship between areas of contact calculated by Hertz's equation and Young's modulus of metal. In this case the metal rider is in contact with silicon carbide. The area of contact A is nearly given by the expression $A = KE_1^n$. The power n depends on the Young's modulus of metal. As anticipated from equation (4), the $-2/3$ power was obtained with the metals having low Young's moduli, such as yttrium to titanium. (See fig. 3.) The value of n is approximately -0.6 for palladium to chromium and -0.5 for molybdenum to iridium.

The ideal tensile strengths for most metals are given as a function of $E^{1/2}$ with exceptions of low Young's moduli metals such as yttrium, aluminum, zirconium, and titanium (fig. 4).

Thus, the decrease in the contact area, with an increase of Young's modulus, is generally greater than the increase in the ideal tensile strength σ_{max} with E. Consequently, the force F required to move the solid rider in a direction parallel to the surface of solid flat decreases with increasing Young's modulus. This fact is consistent with the results of figure 2.

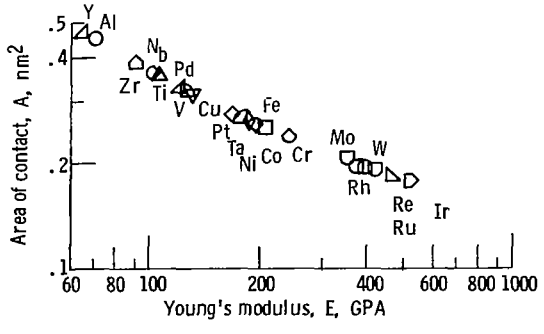

Figure 3. - Area of contact between metal and silicon carbide as function of Young's modulus.

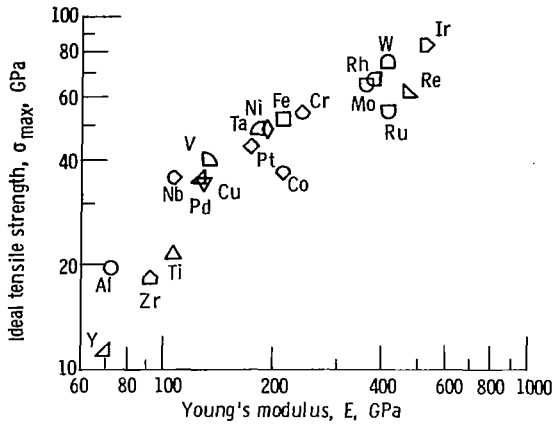

Figure 4. - Ideal tensile strength of metal as function of Young's modulus.

On separation of the metallic and nonmetallic material in sliding contact, tearing and shearing fracture occurs in the metal as well as the shearing at the adhesive bonds in the interface. Morphology of metal transfer to the nonmetal revealed that the metals that have low tensile strength exhibit much more transfer than those that have higher tensile strength (ref. 5). The areas of metal transfer for the metals of low Young's moduli, such as titanium and aluminum, are generally larger than the apparent area of contact, while those for the metals of high Young's moduli, such as tungsten and rhodium, are smaller than the apparent area of contact.

In the case for the metals that have low tensile strength, the actual force F required to move the solid rider in a direction parallel to the surface of the solid flat is higher than the estimated value calculated from equation (2) using the apparent area of contact, because the true fracture area during sliding is larger than the apparent area of contact.

In the case for the metals that have high tensile strength, the actual force F is lower than the estimated value calculated from equation (2) using the apparent area of contact, because the fracture area is smaller than the apparent area of contact. These facts can also help to understand the results of figure 2.

Such dependency of metal transfer on the ideal tensile strength or Young's modulus arises from the adhesion and fracture properties of the metal. The adhesion properties of metals may relate to the chemical activity of metals; for example, titanium is more active, and rhodium is less active (refs. 2 to 6).

Thus, the ideal tensile strengths as functions of the surface energy, Young's modulus, and interplanar spacing of crystal, play two roles in the adhesion and friction of metals contacting nonmetals or metals contacting themselves.

Further correlations between surface energy and other physical properties have been sought by many authors (refs. 12, 13, and 19). The most successful and widely accepted of these correlations for elemental solids is that where the heat of sublimation has been considered. A good correlation between surface and cohesive energy was also found by Tyson and Jones (refs. 12 and 13).

Summary of Results

An estimate of the ideal uniaxial tensile strength σ_{max} was obtained in terms of the equilibrium surface energy and interplanar spacing of the planes perpendicular to the tensile axis and the appropriate Young's modulus.

The adhesion and friction properties of metals in contact with diamond, boron nitride, silicon carbide, manganese-zinc ferrite, and metals were examined in a vacuum of 10^{-8} pascal at low sliding speed.

The coefficients of friction for metals were related to the ideal tensile strengths of metals. The higher the strength of the metal, the lower the coefficient of friction.

Lewis Research Center
National Aeroutics and Space Administration
Cleveland, Ohio, February 9, 1981

References

1. Pauling, L.: A Resonating-Valence-Bond Theory of Metals and Intermetallic Compounds. Proc. Roy. Soc. (London), Ser. A, vol. 196, no. 1046, Apr. 1949, pp. 343–362.
2. Buckley, Donald H.: The Metal-to-Metal Interface and Its Effect on Adhesion and Friction. J. Colloid Interface Sci., vol. 53, no. 1, Jan. 1977, pp. 36–53.
3. Miyoshi, Kazuhisa and Buckley, Donald H.: Adhesion and Friction of Single-Crystal Diamond in Contact with Transition Metals, Applications of Surface Science, vol. 6, 1980, pp. 161–172.
4. Buckley, Donald H.: Friction and Transfer Behavior of Pyrolytic Boron Nitride in Contact with Various Metals. ASLE Trans., vol. 21, no. 2, Apr. 1978, pp. 118–124.
5. Miyoshi, Kazuhisa and Buckley, Donald H.: Friction and Wear Behavior of Single-Crystal Silicon Carbide in Sliding Contact with Various Metals. ASLE Trans., vol. 22, no. 3, July 1979, pp. 245–256.
6. Miyoshi, Kazuhisa and Buckley, Donald H.: Friction and Wear of Single-Crystal Manganese-Zinc Ferrite. Wear, vol. 66, 1981, pp. 157–173.
7. Gilman, John J.: Cleavage, Ductility, and Tenacity in Crystals. Fracture, B. L. Auerbach, D. K. Felbeck, G. T. Hahn, and D. A. Thomas, eds., MIT Press and John Wiley and Sons, Inc., 1959, pp. 193–224.
8. Polanyi, M.: Uber die Natur des Zerre, Bvorganges. Z. Phys. vol. 7, 1921 pp. 323–327.
9. Orowan, E.: Mechanical Cohesion Properties and the "Real" Structure of Crystals. Z. Krist. vol. 89, no. 3–4, Oct. 1934, pp. 327–343.
10. Orowan, E.: Fracture and Strength of Solids. Rep. Prog. Phys., vol. 12, 1948–49, pp. 185–232.
11. Orowan, E.: Energy Criteria of Fracture. Weld. J. vol. 34, Mar. 1955, pp. 157S–160S.
12. Tyson, W.R.: Surface Energies of Solid Metals. Can. Metall. Q., vol. 14, no. 4, 1975, pp. 307–314.
13. Jones, H.: The Surface Energy of Solid Metals. Met. Sci. J., vol. 5, 1971, pp. 15–18.
14. Murr, L. E.: Interfacial Phenomena in Metals and Alloys. Addison-Wesley Publ. Co., 1975.
15. Overbury, S. H.; Bertrand, P. A.; and Somorjai, G. A.: Surface Composition of Binary Systems; Prediction of Surface Phase Diagrams of Solid Solutions. Chem. Rev., vol. 75, no. 5, 1975, pp. 547–560.
16. Eustathopoulos, N.; Joud, J. C., and Desre, P.: Interfacial Tension of Pure Metals. I—Estimation of the Liquid-Vapor and Solid-Vapor Surface Tensions From the Cohesion Energy. II—Estimation of the Solid-Vapor and Solid-Liquid Interfacial Tensions From the Surface Tension of Liquid Metals. J. Chim. Phys. Physicochim. Biol., vol. 70, no. 1, 1973, pp. 38–49.
17. Linford, R. G.: Surface Thermodynamics of Solids. Solid State Surface Science II, M. Green, ed., Marcel Dekker, 1973, pp. 1–152.
18. Roth, T. A.: Surface and Grain-Boundary Energies of Iron, Cobalt and Nickel. Mater Sci. Eng. vol. 18, no. 2, 1975, pp. 183–192.
19. Miedema, A. R.: Surface Energies of Solid Metals. Metallk., Band 69 H5, May 1978, H5, pp. 287–292.
20. Winterbottom, W. L.: Crystallographic Anisotropy in the Surface Energy of Solids. Surfaces and Interfaces, Vol. 1, Chemical and Physical Characteristics, J. J. Burke, N. L. Reed, and V. Weiss, eds., Syracuse Univ. Press, 1967, pp. 133–165.
21. Tyson, W. R.; Ayres, R. A.; and Stein, D. F.: Anisotropy of Cleavage in b.c.c. Acta Metall; Transition Metals. vol. 21, May 1973, pp. 621–627.
22. Basterfield, J.; Miller, W. A.; and Weatherly, G. C.: Anisotropy of Interfacial Free Energy in Solid-Fluid and Solid-Solid Systems. Can. Metall. Q., vol. 8, no. 2, 1969, pp. 131–144.
23. Gschneidner, Karl A., Jr.: Physical Properties and Interrelations of Metallic and Semimetallic Elements. Solid State Physics, Vol. 16, F. Seitz and D. Turnbull, eds., Academic Press, 1964, pp. 275–426.
24. Barrett, Charles Sanborn: Structure of Metals. Crystallographic Methods, Principles, and Data. McGraw-Hill Book Co., Inc., 1943, pp. 552–554.
25. Lyman, Taylor, Ed.: Metals Handbook. Vol. 1: Properties and Selection of Metals, Eight ed., American Society for Metals, 1961.
26. Bowden, F. P.; and Tabor, D.: The Friction and Lubrication of Solids. Clarendon Press (London), 1950.

1. Report No. NASA TP-1883	2. Government Accession No.	3. Recipient's Catalog No.
4. Title and Subtitle RELATIONSHIP BETWEEN THE IDEAL TENSILE STRENGTH AND THE FRICTION PROPERTIES OF METALS IN CONTACT WITH NONMETALS AND THEMSELVES		5. Report Date September 1981 6. Performing Organization Code 506-53-12
7. Author(s) Kazuhisa Miyoshi and Donald H. Buckley		8. Performing Organization Report No. E-587 10. Work Unit No.
9. Performing Organization Name and Address National Aeronautics and Space Administration Lewis Research Center Cleveland, Ohio 44135		11. Contract or Grant No. 13. Type of Report and Period Covered Technical Paper
12. Sponsoring Agency Name and Address National Aeronautics and Space Administration Washington, D.C. 20546		14. Sponsoring Agency Code
15. Supplementary Notes		

16. Abstract

The relationship between the ideal tensile strength and friction properties of metals in contact with diamond, boron nitride, silicon carbide, manganese-zinc ferrite, and the metals themselves in vacuum was investigated. An estimate of the ideal uniaxial tensile strength σ_{max} was obtained in terms of the equilibrium surface energy, interplanar spacing of the planes perpendicular to the tensile axis, and the Young's modulus of elasticity. The coefficient of friction for metals was found to be related to the ideal tensile strength of metals: The higher the strength of the metal, the lower the coefficient of friction.

17. Key Words (Suggested by Author(s))
Tribology
Friction
Tensile strength
Metals

18. Distribution Statement
Unclassified - unlimited
STAR Category 27

19. Security Classif. (of this report)	20. Security Classif. (of this page)	21. No. of Pages	22. Price*
Unclassified	Unclassified	9	A02

* For sale by the National Technical Information Service, Springfield, Virginia 22161

NASA-Langley, 1981

National Aeronautics and
Space Administration

Washington, D.C.
20546

Official Business
Penalty for Private Use, $300

SPECIAL FOURTH CLASS MAIL
BOOK

Postage and Fees Paid
National Aeronautics and
Space Administration
NASA-451

2 1 1U,C, 092481 S00903DS
DEPT OF THE AIR FORCE
AF WEAPONS LABORATORY
ATTN: TECHNICAL LIBRARY (SUL)
KIRTLAND AFB NM 87117

NASA

POSTMASTER: If Undeliverable (Section 158 Postal Manual) Do Not Return